Global J. Environ. Sci. Manage. 10(1): 83-96, Winter 2024, Serial #37

Global Journal of Environmental Science and Management
(GJESM)

Homepage: https://www.gjesm.net/

Podcasts

ORIGINAL RESEARCH PAPEER

Wetland degradation monitoring using multi-temporal remote sensing data and watershed land degradation index

I. Ridwan[1,*], S. Kadir[2], N. Nurlina[1]

[1] *Geophysics, Lambung Mangkurat University, Jl. Ahmad Yani km 36, Banjarbaru, South Kalimantan, Indonesia*

[2] *Forest Faculty, Lambung Mangkurat University, Jl. Ahmad Yani km 36, Banjarbaru, South Kalimantan, Indonesia*

ARTICLE INFO

Article History:
Received 17 March 2023
Revised 24 May 2023
Accepted 30 July 2023

Keywords:
Land degradation index
land use/land cover (LULC)
Soil erosion
Soil moisture content
Vegetation coverage

DOI: 10.22034/gjesm.2024.01.07

ABSTRACT

BACKGROUND AND OBJECTIVES: The condition of the watershed area, particularly the Tabunio Watershed, is one with priority treatment due to the condition of the land where it is located, which qualifies for the “very high recovery” category with a critical land area of 19,109.89 hectares. Moreover, the diminishing water absorption also results in flooding during the rainy season and drought in the dry season. Environmental damage in the Tabunio Watershed is exacerbated by the existence of traditional gold mining and has become a concern for many parties. With this in mind, the perceived increase in natural disasters, such as floods, landslides, and droughts from year to year requires an evaluation of land degradation in the Tabunio Watershed.
METHODS: The objective of this study was to monitor and simulate the spatial and temporal aspects of land degradation in the Tabunio Watershed. It was suggested that a complete land degradation index be developed to capture the spatial and temporal aspects of land degradation between the years 2005 and 2020. This index integrates land use land cover, vegetation coverage, soil erosion, and soil moisture content.
FINDINGS: The proposed comprehensive land degradation index in this study demonstrated that (a) the land degradation index, which successfully monitored the spatio-temporal aspect of land degradation (kappa coefficient > 0.73 and overall accuracy > 86 percent), is regarded as having high accuracy. (b) In comparison to the individual indices, the land degradation index is capable of revealing land degradation in a more comprehensive manner. (c) land degradation index is readily transferable and applicable to other study areas due to the fact that all of its land degradation indices can be quickly extracted from remotely sensed imagery. (d) land degradation index can be used in a wide variety of contexts, which also accounts for the provision of quantitative predictions with regard to the possibility of land degradation. (e) The rate of land degradation will generally increase from 2005 to 2020, with 2010 being the most extreme year.
CONCLUSION: The proposed comprehensive land degradation index method is capable of describing the spatial and temporal aspect of land degradation from 2005 to 2020 in the watershed area. Moreover, the proposed approach shows that the level of land degradation from 2005 to 2020 normally increases, recording the extreme years as the 2010s. In addition, in most years, the amount of land degradation was moderate, only few of which had severe or extreme degradation. As a consequence of this, some land degradation management measures ought to be created in advance, guaranteeing the protection of this vital region, which is a source of freshwater. The study provides a substantial understanding of the effect of land degradation on sustainable environment management and development in the watershed.

NUMBER OF REFERENCES	NUMBER OF FIGURES	NUMBER OF TABLES
62	3	3

*Corresponding Author:
Email: *ichsanridwan@ulm.ac.id*
Phone: +813 5103 7167
ORCID: 0000-0002-8739-5038

Note: Discussion period for this manuscript open until April 1, 2024 on GJESM website at the “Show Article”.

INTRODUCTION

The resources provided by the land constitute an essential component of the material basis for human existence and advancement. In recent years, the irresponsible use of land resources, combined with the poor management of those resources, as well as the growth of the world's population, has led to severe land degradation across the globe (Ahmad and Pandey, 2018; Zhu *et al.,* 2022, Suharyanto *et al.,* 2023). The condition of the watershed area, particularly the Tabunio Watershed, is one with priority treatment due to the condition of the land where it is located, which qualifies for the "very high recovery" category with a critical land area of 19,109.89 hectare (ha). Moreover, the diminishing water absorption also results in flooding during the rainy season and drought in the dry season (Takrina *et al.,* 2023; Enriquez and Tanhueco, 2022). In the last three years, Tanah Laut Regency has frequently become a casualty of flooding. The worst of which occurred in 2021, causing the submergence of approximately 107 residents' houses in floods as deep as two to three meters. The catastrophe also caused damage to the main road, obstructing the in-and-out road access to Tanah Laut Regency. The floods are suspected to be brought about by the environmental degradation due to the hundreds of un-reclaimed mining pits, of which, 50 percent (%) of the 3.7 million hectares of land are controlled by mining and palm oil companies. Environmental damage in the Tabunio Watershed is exacerbated by the existence of traditional gold mining and has become a concern for many parties. With this in mind, the perceived increase in natural disasters, such as floods, landslides, and droughts from year to year requires an evaluation of land degradation in the Tabunio Watershed, which is one of the most important sources of freshwater in the Tanah Laut Regency. Land degradation, often manifested in soil erosion, the loss of quality farmland, and the fall of plant coverage, is affecting the water quality as well. Although Tabunio Watershed is one of the most important supply in Tanah Laut Regency, its water quality continues to be negatively impacted. The degradation of land can have a wide range of negative effects on the surrounding environment, including the amplification of soil loss, a decline in biodiversity, a deterioration in the ecosystem, and a loss in the land's capacity to be used for other purposes (Dubovyk, 2017; Faisal *et al.,* 2019). Since addressing land degradation effectively is crucial, in 2015 the United Nations applied the "Sustainable Development Goals," one of which consists of combating and restoring degraded land (Dubovyk, 2017; Moonrut *et al.,* 2021). The steps to address land degradation in the affected watersheds (DAS) require a structured approach, involving various stakeholders. One of them is utilizing mapping and field surveys in the identification of areas within the watershed that are experiencing land degradation. This will help prioritize which areas require urgent restoration and conservation actions. This goal aims to achieve land degradation neutrality by the year 2030. The mitigation of climate change and the conservation of biodiversity, as well as the improvement of food security and the upkeep of sustainable livelihoods, all benefit from the management of land degradation (Tolche *et al.,* 2022; Frimawaty *et al.,* 2023). The use of remote-sensing techniques has become increasingly common in the field of land degradation research due to the fact that these techniques have many benefits, including the ability to detect land degradation of varying degrees (Ejegu *et al.,* 2022; Kumsa and Assen, 2022; Shange, 2020); as well as the capability of locating and mapping land degradation. At the moment, there are four major steps in the process of using remote-sensing methods to evaluate land degradation (Gashaw *et al.,* 2014; Hu *et al.,* 2020). Numerous studies use a combination of indices to indicate land degradation—for example, the normalized difference vegetation index (NDVI), soil erosion (SE) (Ghobadi *et al.,* 2012; Kumsa and Assen, 2022), land use/cover change (Gashaw *et al.,* 2014; Moonrut *et al.,* 2021; Van Lynden and Mantel, 2001), and land degradation (Ibrahim *et al.,* 2015). The accuracy of the monitoring cannot be verified in a satisfactory manner. As a result, improving the precision of land-degradation monitoring and creating a comprehensive index of land degradation are both urgent requirements. The ability to simulate and predict the degradation of land can provide important information that can help guide decision-making. The Markov model, System dynamics (SD), modified universal soil loss equation (MUSLE), and multi-agent model are some of the simulation and prediction models that are widely employed in the research on land degradation. MUSLE, as well as an erosion and sedimentation prediction tool called

EROSET (Borrelli *et al.,* 2021; Karydas *et al.,* 2014; Ly *et al.,* 2019; Wiratmoko and Gunawan, 2019). However, it is important to note that none of these models are foolproof, and majority of them concentrate on simulating changes in land use or land cover or on simulating individual indicators of land degradation. In addition, only a few of these models are used to simulate land degradation in its entirety (Borrelli *et al.,* 2021; Febrianti *et al.,* 2018; Karaburun, 2010; Karydas *et al.,* 2014). Quantitatively predicting a dynamic change in landscape characteristic is within the capabilities of Markov models, but these models are incapable of resolving the spatial characteristic of landscape change (García *et al.,* 2019; Liping *et al.,* 2018; MohanRajan and Loganathan, 2021; Oguz and Zengin, 2011). The CA model can predict where the landscape pattern would appear, but it can't tell us when it will change (Liping *et al.,* 2018; MohanRajan and Loganathan, 2021; Oguz and Zengin, 2011). In light of these considerations, it is essential to integrate a variety of modeling approaches to successfully simulate the spatial and temporal characteristics of land degradation. For instance, the CA-Markov model has the ability to simulate the spatio-temporal dynamics of land degradation and has numerous applications in a variety of scientific communities (Mariye *et al.,* 2022; Tadese *et al.,* 2020; Zhu *et al.,* 2022). Despite the satisfactory results that remote sensing and geographic information systems (GIS) have generated in studies of land degradation (Auliana *et al.,* 2018; Kadir and Farma, 2017), commonly used land degradation indices are inadequate because they do not accurately capture the full range of the severity and the temporal and spatial dimensions of land degradation (Zhu *et al.,* 2022). It is necessary to have an integrated remote-sensing index that can track the spatial and temporal features of land degradation to provide coverage for the aforementioned indices. Understanding of the spatial and temporal characteristics of land degradation as well as the factors that cause it, with the goal of improving environmental protection, is a necessity for the case of the Tabunio Watershed. The findings of this study can provide baseline information that can be used in preserving the environmentally sound development of this watershed ecosystem. The purpose of this research is to create an extensive land degradation index (LDI) by combining indices from multiple remote-sensing sources in the evaluation of the spatial and temporal aspects of land degradation. This study has been carried out in the Tabunio Watershed from 2005 to 2020.

MATERIALS AND METHODS

Study area

The Tabunio Watershed (3°37'2.72"-3°51' 51.43" SL and 114°36' 12.02"114°57'47.62" EL) is located in Tanah Laut Regency. It has an area of approximately 62,558.56 ha and dominated the area with the lowest elevations. The Tabunio Watershed is shown in Fig. 1. It is not only an essential resource for the economic and social growth of Tanah Laut Regency in a sustainable manner but is also a water resource for the Riam Kanan Dam. The land resources in the Tabunio Watershed are rapidly deteriorating as a result of both natural and human-caused changes in the surrounding environment, drawing an increasing amount of attention to the need for mitigation.

Data source

The multispectral image of the research region, which was taken on January 20 and did not contain any clouds, was retrieved from The Glovis United State of Geologycal Survey. These data were captured by LANDSAT ETM+ in year 2005 and 2010 and LANDSAT 8 OLI (2015 and 2020). These images have a spatial resolution of 30 meters, six or eight bands at visible and shortwave wavelengths, and one panchromatic band with a resolution of 15 meters (for ETM+ and OLI). ETM+ images have eight spectral bands, while the OLI image only has one. The historic rainfall, relative humidity, and temperature data for January 20 were downloaded from the Center of Hidrometeorology and Remote Sensing (CHRS). The images from the years 2005, 2010, 2015, and 2020 were used for the study. The digital vector data can be found at the following location: Tabunio Watershed administration provided us with a soil-type map, a scale of 1:125.000, and data on land use planning for the Tabunio Watershed.

Methods

The following methodical structure was developed in this research for the purpose of tracking and predicting the degradation of land. It includes the creation of an LDI, the evaluation of the risks associated with land degradation, as well as the observation and simulation accuracy assessments.

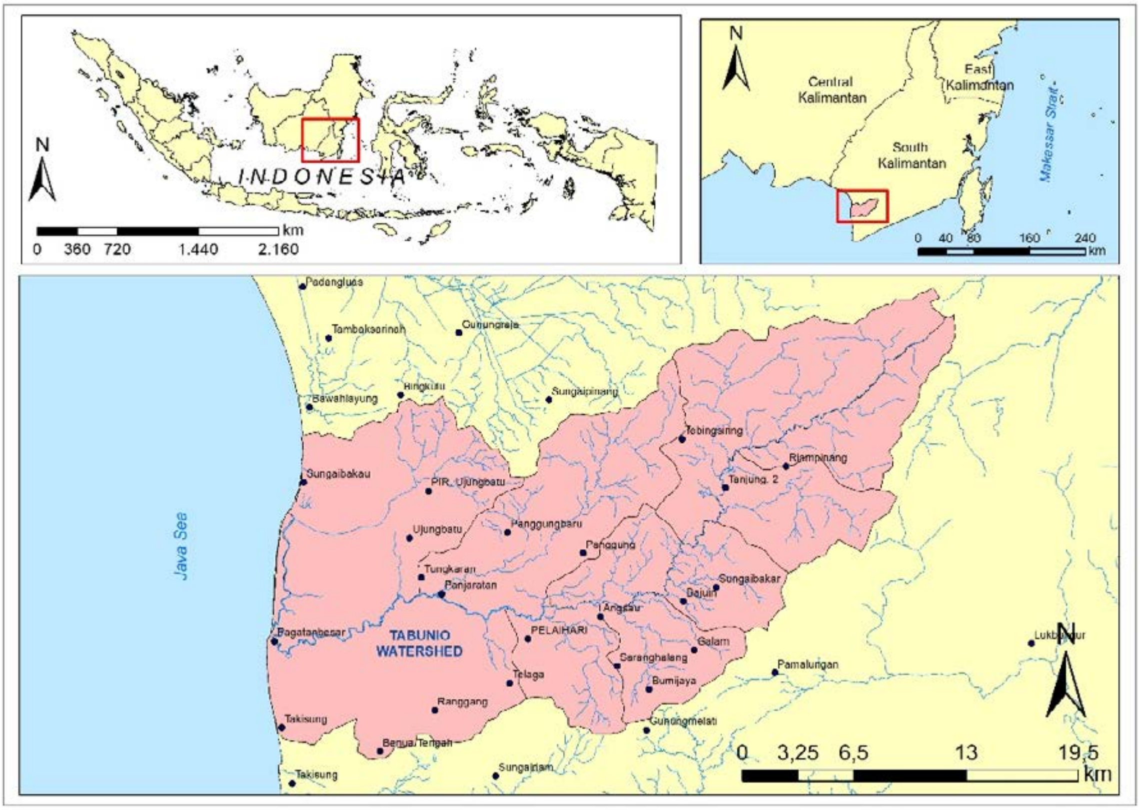

Fig. 1: Geographical location of the study area in the Tabunio Watershed, South Kalimantan, Indonesia.

The most common variety of land degradation are soil erosion, decreased soil fertility, soil pollution, forest degradation, salinization, desertification and urbanization (Loukrakpam and Oinam, 2021). These types of land degradation are primarily responsible for four indicators that describe land degradation, chosen according to actual conditions observed in the field in the Tabunio Watershed. These indicators are land use land cover, vegetation coverage, soil erosion, and soil moisture content.

Land use land cover (LULC)

LULC was chosen to be one of the indices used to describe land degradation because changes in LULC are one of the most significant factors that contribute to land degradation in the Tabunio Watershed. For the preprocessing of the LANDSAT TM/ETM+/OLI images that were downloaded, the ENVI 5.3 software was utilized, accomplishing the band combined, FLAASH atmospheric adjustment, combining images, and image selection were all. This technique has the potential to improve the spatial accuracy of a multispectral bands while maintaining the accuracy of the spectral information included in the source data. The land-use classification process begins with the determination of the land cover/use class based on the dominant land cover in the Tabunio Watershed. This study divides land use into 10 classes, including bodies of water, forests, open land, settlements, plantations, agriculture, swamps, shrubs, ponds, and mines. Then the process of land-cover classification is carried out. Moreover, the classification method used in this study is the support vector machine (SVM) method, which was chosen for its high accuracy (OA > 80%) (Nurlina *et al.,* 2021). Each image was initially categorized into one of ten different LULC types. These LULC types were then arranged in descending order of the likelihood of land degradation, starting from the least likely to the most likely scenario. When looking at the LULC types, a higher score indicates that there is a greater likelihood of land degradation. The order of the score is as follows: water body, forest, pond, swamp, plantation, agriculture, settlement, shrubs, bare land, and mining.

Vegetation coverage

There is a one-to-one correlation between the state of the vegetation cover and the level of land degradation (Aires *et al.,* 2020; Fang *et al.,* 2021; Sun *et al.,* 2020). The composite vegetation index (CVI), a significant metric of vegetation density, was determined in this study using the forest canopy density (FCD) mapping approach. The model is dependent on vegetation indices, and the indices that are generally used to generate the canopy vegetation index (CVI) are the normalized difference vegetation index (NDVI), the shadow index (SI), and the bare soil index (BI), using Eqs. 1-3 (Godinho *et al.,* 2016; Loi *et al.,* 2017; Su Mon *et al.,* 2012)

$$CVI = \left(NDVI + nBI \right) * SI \tag{1}$$

$$VC = \frac{\left(CVI - CVI_{soil} \right)}{\left(CVI_{veg} - CVI_{soil} \right)} , \tag{2}$$

Where, CVI_{veg} and CVI_{soil} represent CVI values of vegetation cover and bare soil cover, and using Eqs. 3-5 (Godinho *et al.,* 2016; Loi *et al.,* 2017):

$$NDVI = \frac{\rho_{NIR} - \rho_{RED}}{\rho_{NIR} + \rho_{RED}} NDVI = \frac{\rho_{NIR} - \rho_{RED}}{\rho_{NIR} + \rho_{RED}} \tag{3}$$

$$SI = \left[\left(256 - \rho_{BLUE} \right) \left(256 - \rho_{GREEN} \right) \left(256 - \rho_{red} \right) \right]^{1/3} \tag{4}$$

$$BI = \frac{\rho_{swir} + \rho_{RED} - \rho_{NIR} - \rho_{BLUE}}{\rho_{swir} + \rho_{RED} + \rho_{NIR} + \rho_{BLUE}} \tag{5}$$

Where, BLUE, GREEN, RED, NIR, and SWIR each stand for the reflectance of LANDSAT images in the blue band, the green band, the red band, the near-infrared band, and the first shortwave infrared band. According to the FCD model, the percentage of land covered in vegetation has a positive correlation with SI and NDVI but a negative correlation with BI. CVI can reduce the effect of shadow and soil background.

Soil erosion (SE)

SE is a complicated physical process that is affected by a wide range of variables. Some of these variables include precipitation (R), soil erodibility (K), slope (S), vertical continuity (L), plant management (C), land conservation efforts (P) and correction factor 0.6 (f) were used to extract SE values using Eq. 6 (Borrelli and Schütt, 2014; Mariye *et al.,* 2022; Nurlina *et al.,* 2022). Rainfall data, vegetation density, length slope, and land use types were extracted from satellite data and digital elevation model.

$$SE = (R * K * L * S * C * P) * f \tag{6}$$

Soil moisture content (SMC)

The SMC is a direct indicator of drought intensity; hence, increasing SMC can help reduce the severity of land degradation (Peng *et al.,* 2020; Perdana *et al.,* 2020; Tajudin *et al.,* 2021). NDVI was integrated with historical temperature data by utilizing an algorithm called a mono-window algorithm, which was done to identify the land surface temperature (LST) of the area that was being researched (El Garouani *et al.,* 2021; Fashae *et al.,* 2020; Guha and Govil, 2021; Nurlina *et al.,* 2023). SMC was calculated using the temperature-vegetation drought index (TVDI) (Eqs. 7–9) in this study. This index is based on the TS-NDVI principle, using Eqs. 7, 8, and 9 (Peng *et al.,* 2020; Wang *et al.,* 2020; Younis and Iqbal, 2015).

$$SMC \approx TVDI = \frac{Ts - Ts_{min}}{Ts_{maks} - Ts_{min}} \tag{7}$$

$$Ts_{maks} = a_1 + b_1 * NDVI \tag{8}$$

$$Ts_{min} = a_2 + b_2 * NDVI , \tag{9}$$

Where, T_S, T_{Smin}, and T_{Smax} each describe the temperature of the land surface of a single pixel in Kelvin (K), the maximum and minimum surface temperatures that correspond to NDVI (K). The coefficients for the dry edge equation and the wet edge equation are a_1, b_1, a_2, and b_2.

Land degradation risk assessment

The relative importance of each indices that have been previously mentioned was determined by comparison, in accordance with the analytical hierarchy process (AHP) principle. The scoring of all variable in the LDI valuation matrix were calculated from expert judgment using a questionnaire. (Anh *et al.,* 2014; Ardali, 2016; Kang *et al.,* 2016; Sar *et al.,* 2015; Vaishali and Patil, 2015). The weights of land use, vegetation coverage, soil erosion, and soil moisture content were computed with AHP Software using Eqs. 10 and 11.

$$IDL = w_a LULC + w_b VC + w_c SE + w_d SMC \tag{10}$$

$$W = (w_{TL}, w_{TV}, w_{ET}, w_{KT})^T = (0.34, 0.30, 0.29, 0.10)^T , \tag{11}$$

Where, w_a, w_b, w_c, and w_d, each stand for the respective weights of land use, vegetation coverage, soil erosion, and soil moisture. As a result of the valuation matrix having a consistency of CR = 0.0121 0.1, the requirements for this study were successfully met.

Following are some of the findings that emerged from our investigation of several indices: (a) the level of LDI increase when the values of land use and soil erosion increased (b) the level of LDI decreased when the rates of vegetation coverage and soil moisture increased. Because of this, to simplify the calculations, the amounts of VC and SMC were standardized using Eq. 12 (Pratt *et al.,* 2004).

$$X = \frac{x_i - x_{min}}{x_{max} - x_{min}} ; X = \frac{x_{max} - x_i}{x_{max} - x_{min}} , \tag{12}$$

Where, X is the normalized value of x_i, x_{min}, and x_{max} are the lowest and highest value of the variable; and X is the value that has been normalized.

Each of the indices that were derived from this process has a value that rises as the amount of degraded land increases. It is intended to reflect the level of land degradation (Eq. 11). Eq. 12 was used to normalize the LDI value so that it falls within the range [0, 1], and a higher LDI value indicates a more severe level of land degradation. Land degradation analysis uses a geographic information system through an overlay process of the four parameters of the LDI with their respective weights and scores (Table 1). LDI values were used to categorize the level of land degradation into five distinct levels, and equal intervals were used for each category. This was done so that it would be easier to compare different years (Table 2 and Fig. 2).

Table 1. Weight value and LDI parameter scoring

Parameter	Weight	Class	Description	Scoring
Land use/land cover	0.3361	Water body		1
		Forest		1
		Bare land		5
		Residential		4
		Plantation		3
		Agriculture		3
		Swamp		2
		Shrubs		4
		Pond		2
		Mining		5
Soil erosion (t/ha/yr)	0.2869	< 15	Very light	1
		15–60	Light	2
		60–180	moderate	3
		180–480	Heavy	4
		> 480	Very heavy	5
Vegetation coverage	0.2802	0–0.2	Not vegetation	5
		0.2–0.4	Vegetation is very sparse	4
		0.4–0.6	Sparse vegetation	3
		0.6–0.8	Dense vegetation	2
		0.8–1	The vegetation is very dense	1
Soil moisture content	0.0968	< 0.2	Very wet	1
		0.2–0.4	Moist	2
		0.4–0.6	Slightly moist	3
		0.6–0.8	Slightly dry	4
		> 0.8	Dry	5

Table 2. LDI Value (Tolche *et al.,* 2022)

LDI Value	Class degradation	Description
0–0.4	No degradation	No degradation, which includes water, areas of complete vegetative cover, building areas, and arable land with high fertility.
0.2–0.4	Mild degradation	The mild degradation is one in which agricultural output has dropped but ecosystem services have not been compromised.
0.4–0.6	Moderate degradation	There has been a moderate decline in land production and some harm to ecosystem function in a region classified as moderately degraded.
0.6–0.8	Severe degradation	The severe degradation category refers to a region that has suffered significant losses in terms of both land production and ecosystem function.
0.8–1	Extreme degradation	Extreme land degradation is characterized by the loss of all land production and ecosystem function.

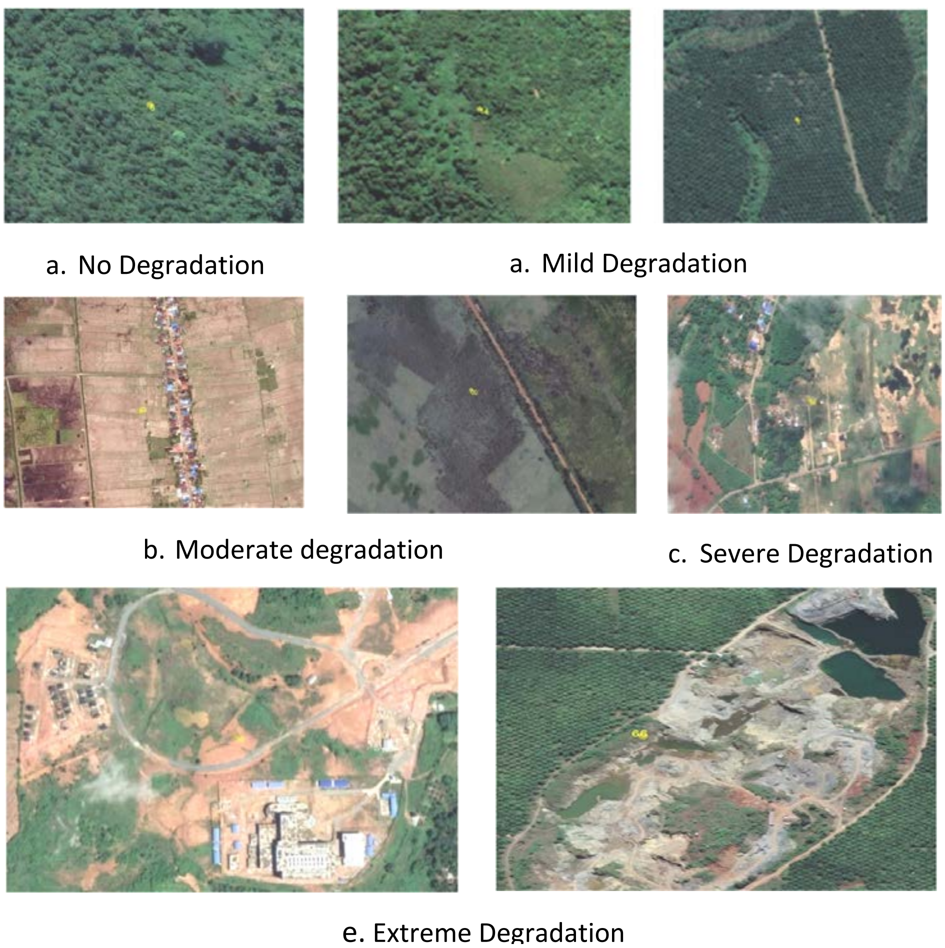

Fig. 2: The characteristics of land degradation validation samples

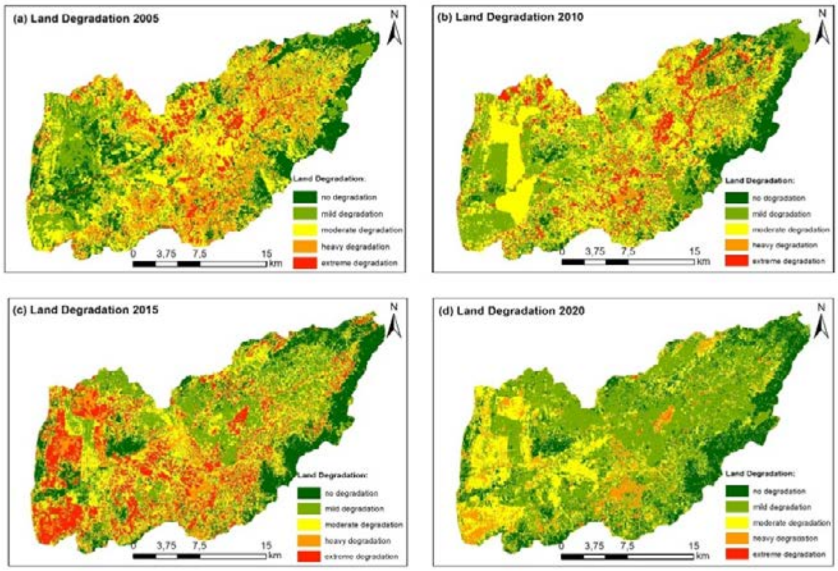

Fig. 3: Spatial and temporal distribution of land degradation index in study area

RESULTS AND DISCUSSION

The results of the land-cover classification process from 2005 to 2020 show changes in land use as a whole. There are four types of land cover that changed very rapidly with quite significant changes, namely, an increase in the area of plantation land cover followed by a decrease in shrubs and agricultural land and swamp land cover. The positive land use and land cover changes observed in the Tabunio Watershed are a significant increase in the area of plantations, from 502.16 ha in 2005 to 24,313.31 ha in 2020—an increase of 23,811.15 ha (4,841%) and a decrease in the mining area from 2,172.66 ha in 2005 to 350.50 ha in 2020, decreasing by 1,822.17 ha (619.8%) (Nurlina *et al.,* 2021).

Monitoring and evaluation of land-degrading conditions

Fig. 3 shows how the rates of land decline in the Tabunio Watershed changed over the time period of 2005 to 2020. It is split into five levels: areas with no degradation, mild degradation, moderate degradation, serious degradation, and extreme degradation. The degree of land degradation was determined by the area and percentage of LDI in each class.

Spatio-temporal distribution of LDI (Fig. 3), showed that no degradation areas are found in land cover, bodies of water, and forests, while degradation land are evenly distributed in mining areas, bare land, agricultural land, and plantations with steep and gentle slopes around the Tabunio Watershed. In 2015, most of the areas with severe and extreme LDI were in the south and west areas, and most of them with mild and moderate LDI were in the hilly and plantation zones around the upstream watershed. In terms of the patterns and measurements of land degradation in the Tabunio Watershed, it usually worsened from 2005 to 2020, with the amount of degraded land reduced steadily from 2015 to 2020 except on the years 2005 and 2010. Between the years 2005 and 2015, there was a significant increase in the amount of land that was degraded, which was greater than 50,000 hectares (ha) and 53%. The degree of land degradation underwent drastic changes in 2015–2020; and specifically, the area undegraded increased from 12% in 2010 to 17% in 2015, with an increase in area of 3,271 ha (Table 3); severed degradation decreased from 24,352 ha (38.93%) and 11,810 ha (18.88%) in 2015 to 14,416 ha (23%) and 226.2 (0.36%) in 2020. Total degraded land remains at or beneath 50,000 ha. In terms of the level of land degradation, light to severe land degradation was observed almost throughout the year, while

Table 3: Proportion of land degradation in the Tabunio Watershed from 2005 to 2020

Degradation Class	2005		2010		2015		2020	
	Area (ha)	Proportion (%)	Area (ha)	Proportion (%)	Area (ha)	Proportion (%)	Area (ha)	Proportion (%)
No degradation	11,266.05	18.01	7,689.62	12.29	10,960.44	17.52	12,282.15	19.63
Mild degradation	15,177.40	24.26	20,638.21	32.99	16,024.79	25.62	30,273.44	48.39
Moderate degradation	21,318.96	34.08	24,352.41	38.93	18,092.33	28.92	14,416.51	23.04
Severe Degradation	8,905.55	14.24	2,908.26	4.65	5,670.68	9.06	5,360.24	8.57
Extreme Degradation	5,890.61	9.42	6,970.05	11.14	11,810.33	18.88	226.22	0.36

the portion of areas with extreme degradation was relatively slight. The rate of land degradation will have dropped by a sizeable amount by the year 2020, and the percentage of land that will be severely and extremely degraded will drop to 9% and 1% (Table 3). Area and proportion of land degradation in the Tabunio Watershed from 2005 to 2020.

The extensive LDI that was proposed in this research proved to be effective in monitoring the spatial and temporal aspects of land degradation (KC > 0.73 and OA > 86%), which is significant when taking into account that a Kappa coefficient that falls within the range of 0.70–0.85 is regarded as having "high accuracy" (Chikhaoui *et al.,* 2005; Ibrahim *et al.,* 2015; Tolche *et al.,* 2022). Even though an accuracy test has been carried out using a confusion matrix, the assessment of the level of land degradation, however, is still subjective, especially for mild and moderate degradation. When compared with individual indices, the LDI is capable of revealing land degradation in a more comprehensive manner. LDI is easily transferable and relevant to various research areas because all of its LDI may be produced quickly from remotely sensed data. As a result, LDI can be used in a wide variety of contexts, making quantitative predictions regarding the possibility of land degradation. In this study, the procedure for deriving the LDI land degradation evaluation matrix was exhaustive, and the assessments matrix was consistent with consistency ratio (CR) is 0.012. This is significant when taking into consideration that a CR of less than 0.1 is considered to be qualified (Atmaja *et al.,* 2019; Solangi *et al.,* 2019). Several studies on land degradation have been estimated quantitatively by analyzing physico-chemical parameters where spatial variability in soil parameters is described through soil maps generated from GIS analysis (Ahmad and Pandey, 2018). Other studies used the following parameters in this study: rainfall; NDVI LST; topography; and pedological properties (i.e., soil depth, soil pH, soil texture, and soil drainage) (Shange, 2020). Another LDI is based on the concept of a soil line derived from spectroradiometric measurements of soil that compares the LDI and degraded spectral angle (SAM) approaches in assessing and estimating land degradation (Chikhaoui *et al.,* 2005). The results shown from several other studies only used a single index and focused more on soil conditions and did not carry out an accuracy test for the LDI. Our research combines four very complete indices, which are composed of 15 single indices (Eq. 1 to Eq. 9) and with the LDI accuracy test. This study area experienced an acceleration in the loss of biodiversity, destruction of vegetation, and loss of water and soil due to the acceleration of tourism and expansion of oil palm plantation. This resulted LDI with significant region and a percentage of land degraded between 2005 and 2020. It is important to note the dramatic shift that occurred in the land degradation classes between the years 2005 and 2005. The local government began implementing the Grain for Green Programme policy at the beginning of 2015. The goal of this policy was to assist in the conversion of bare land and mining back into forest or plantation. This policy reduced the degree to which land was degraded, which may explain why areas with no degradation increased while areas with severe degradation decreased during the 2005–2020 period. The Tabunio Watershed Management Department engaged in a number of protective efforts, such as delimiting development zones, restricting population expansion and greening scenic regions. These policies and measures resulted in a gradual reduce in the rate of land degradation. It is interesting that the amount of rain in the Tabunio Watershed affects the level of SE, and that the level of SE goes up in years when there is a lot of rain. The SE is a significant indicator of land degradation; changes in the SE reflect land degradation to a significant degree. During the years 2005–2020, the annual precipitation in the Tabunio Watershed showed a very slight downward trend. Beginning in the year 2015, this precipitation began a significant downward trend (Nurlina *et al.,* 2022). As a result, the disparity between the amount of precipitation and the amount of water lost to evaporation was a driving force behind the reduction of SE in the Tabunio Watershed from 2005 to 2020, which indicated that land degradation was presenting a trend toward improvement, particularly after the year 2010. The proposed comprehensive LDI approach shows that the land degradation classes of the Tabunio Watershed underwent rapid change during the 2005–2022 period, and the vast majority of the effects of these shifts, in terms of slowing down or even reversing land degradation, were beneficial. Some examples of these positive consequences include the expansion of areas with no degradation and the reduction of areas with severe degradation. The control measures for bettering the management of land degradation still need to be worked on. In light of the findings of an investigation into the causes and effects of land degradation, in conjunction with an examination of the characteristics of the Tabunio Watershed, the following proposals for preventative and corrective actions could be made: (a) minimizing the use of pesticides and chemical fertilizers or switching to organic and (b) recommending that biological or engineering building techniques be used in highly degraded areas, such as a more effective slope area management, terraces to store water to minimize water loss and soil erosion, and more plant life make the rehabilitation program work better (Akumu *et al.,* 2018; Khawaldah *et al.,* 2020).

CONCLUSION

In this study, the proposed comprehensive LDI method is able to describe the spatial and temporal characteristics of land degradation from 2005 to 2020 in *the watershed* area*,* particularly *in the* Tabunio Watershed. The extensive land degaradation index filed in this study combines four major indices that are composed of the presented 15 single indices that were successful in evaluation the spatial and temporal charactersitics of land degradation with Kappa coefficient > 0.73 and overall Accuration > 86%), being regarded as having "high accuracy." The degree to which land was degraded from 2005 to 2020 was, on average, lower than it had been during that time period. The increase in areas with no degradation, as well as the decrease in areas with light and severe degradation, were both positive for the mitigation of land degradation. In comparison to the state of the land in 2005, it was anticipated that the degradation of the land would remain relatively increased in 2005 until 2015. Both natural and anthropogenic factors were responsible for the land degradation that took place in this watershed. The control methods for land degradation should be created based on the results of monitoring and forecasting for the Tabunio Watershed. The suggested approach demonstrates that the level of land degradation generally increased from 2005 to 2020, with the extreme year of land degradation being 2010, and most years' land degradation was moderate, with only a few cases of serious or extreme land degradation. The LDI built from this study shows that the right and very specific combination of variables can produce very good accuracy. Moreover, LD is one of the most serious global threats to people's livelihoods and the environment. At numerous spatial and temporal scales, remote sensing performs an unprecedented role in LD mapping, assessment, and monitoring. Despite the tremendous promise of remote sensing to aid with LD research, a number of problems have hampered its practical implementation, including limited remote-sensing data with high spatial and temporal resolution. A few strategies for preventing further land degradation ought to be established in advance to ensure the protection of this essential region that is a source for freshwater. The research offers a major new understanding of the impact that the degradation of land has on the sustainable management and development of the environment in the watershed.

AUTHOR CONTRIBUTIONS

I. Ridwan, the corresponding author, has contributed in GIS data analysis, interpreted the results, prepared maps, Figures and preparing the manuscript. S. Kadir prepared in vegetation cover data analysis and soil erosion, and interpreted the results. N. Nurlina contributed in remote sensing data analysis, all the field data survey, and manuscript preparation.

ACKNOWLEDGMENTS

The Ministry of Education, Culture, Research, and Technology has funded this study with a National Competitive Applied Research Grant [Number 026/E5/PG.02.00.PL/2023].

CONFLICT OF INTEREST

The authors declare that there is no conflict of interests regarding the publication of this manuscript. In addition, the ethical issues, including plagiarism, informed consent, misconduct, data fabrication and/or falsification, double publication and/or submission, and redundancy have been completely observed by the authors.

PUBLISHER'S NOTE

GJESM Publisher remains neutral with regard to jurisdictional claims with regard to published maps and institutional affiliations.

ABBREVIATIONS

%	Percent
º	Degrees
'	minute
"	second
>	more than
<	less then
AHP	Analytical Hierarchy Process
BI	Bare Soil Index
CHRS	Center of Hidrometeorology and Remote Sensing
CR	Consistency Ratio
CVI	Composite Vegetation Index
DEM	Digital elevation model
EL	East Longitude
ENVI	Environment for Visualizing Images
ETM+	Enhanced Thematic Mapper plus
FCD	Forest Canopy Density
FLAASH	Fast Line-of-sight Atmospheric Analysis of Spectral Hypercubes
GIS	Geographic information system
K	Kelvin
KC	Kappa coefficient
Landsat	Land Satellite
LDI	Land degradation index
LULC	Land use land cover
LST	Land Surface Temperature
MUSLE	Modified universal soil loss equation
NDVI	Normalized difference vegetation index
NIR	Near Infra Red
OA	Overall accuracy
OLI	Operational Land Imager
R	Rainfall erosivity factor
SD	System dynamics
SE	Soil Erosion
SI	Shadow Index
SL	South Latitude
SMC	Soil Moisture Content
SWIR	Short Wave Infra Red
TM	Thematic Mapper
TVDI	Temperature Vegetation Drought Index
USGS	United State Geological Survey
USLE	Universal soil loss equation
VC	Vegetation Cover
ha	hectare

MJ	Mili Joule
mm	milimeter
t	Ton
y	year

REFERENCES

Ahmad, N.; Pandey, P., (2018). Assessment and monitoring of land degradation using geospatial technology in Bathinda district, Punjab, India. Solid Earth. 9(1): 75–90 (**16 pages**).

Aires, U.R.V.; da Silva, D.D.; Moreira, M.C.; Ribeiro, C.A.A.S.; Ribeiro, C.B. de M., (2020). The use of the normalized difference vegetation index to analyze the influence of vegetation cover changes on the streamflow in the Manhuaçu River Basin, Brazil. Water Resour. Manage., 34(6): 1933–1949 (**17 pages**).

Akumu, C.E.; Henry, J.; Gala, T.; Dennis, S.; Reddy, C.; Teggene, F.; Haile, S.; Archer, R.S., (2018). Inland wetlands mapping and vulnerability assessment using an integrated geographic information system and remote sensing techniques. Global J. Environ. Sci. Manage., 4(4): 387–400 (**14 Pages**).

Anh, N.K.; Phonekeo, V.; My, V.C.; Duong, N.D.; Dat, P.T., (2014). Environmental hazard mapping using GIS and AHP – A case study of Dong Trieu District in Quang Ninh Province, Vietnam. IOP Conference Series: Earth Environ. Sci., 18(1): 012045 (**7 pages**).

Ardali, M.R., (2016). Application of remote sensing, GIS and AHP potential water sources (Case study : Anticline shyrogoun). Bulletin of Environment, Pharmacol. Life Sci., 5(7): 63–73 (**11 pages**).

Atmaja, R.R.S.; Putra, D.P.E.; Setijadji, L.D., (2019). Delineation of groundwater potential zones using remote sensing, GIS, and AHP techniques in southern region of Banjarnegara, Central Java, Indonesia. Proceeding of SPIE, 11311 (**11 pages**).

Auliana, A.; Ridwan, I.; Nurlina, N., (2018). Analisis tingkat kekritisan lahan di DAS Tabunio Kabupaten Tanah Laut. Positron. 7(2): 54–59 (**6 pages**).

Borrelli, P.; Alewell, C.; Alvarez, P.; Anache, J.A.A.; Baartman, J.; Ballabio, C.; Bezak, N.; Biddoccu, M.; Cerdà, A.; Chalise, D.; Chen, S.; Chen, W.; De Girolamo, A.M.; Gessesse, G.D.; Deumlich, D.; Diodato, N.; Efthimiou, N.; Erpul, G.; Fiener, P.; Panagos, P., (2021). Soil erosion modelling: A global review and statistical analysis. Sci. Total Environ., 780 146494 (**18 pages**).

Borrelli, P.; Schütt, B., (2014). Assessment of soil erosion sensitivity and post-timber-harvesting erosion response in a mountain environment of Central Italy. Geomorphology. 204: 412–424 (**13 pages**).

Chikhaoui, M.; Bonn, F.; Bokoye, A.I.; Merzouk, A., (2005). A spectral index for land degradation mapping using ASTER data: Application to a semi-arid Mediterranean catchment. Int. J. Appl. Earth Obs. Geoinf., 7(2): 140–153 (**14 pages**).

Dubovyk, O., (2017). The role of Remote Sensing in land degradation assessments: opportunities and challenges. Eur. J. Remote Sens., 50(1): 601–613 (**13 pages**).

Ejegu, M.A.; Reta, K.G.; Yegizaw, E.S.; Biru, B.Z.; Mekonnen, D.M.; Wassie, G.K.; Tegegne, M.A.; Dirar, T.M.; Dubale, Y.G., (2022). Land management, dynamics and vegetation vulnerability analysis in the Guna-Tana watershed as a predictor of land degradation, using remote sensing data. J. Degraded Min. Lands Manage., 9(4): 3703 – 3714 (**12 pages**).

El Garouani, M.; Amyay, M.; Lahrach, A.; Jarar Oulidi, H., (2021). Land Surface Temperature in Response to Land Use/Cover Change Based on Remote Sensing Data and GIS Techniques: Application to Saïss Plain, Morocco. J. Ecol. Eng., 22(7): 100�112 (**13 pages**).

Enriquez, M.D.; Tanhueco, R.M., (2022). A basis water quality monitoring plan for rehabilitation and protection. Global J. Environ. Sci. Manage., 8(2): 237-250 **(14 pages).**

Faisal, A.; Hossain, M.; Haque, S.; Shaunak, M.; Kafy, A., (2019). Remote Sensing Approach in Wetland and Land Degradation Assessment: a Scenario of Modhumoti Model Town, Savar, Bangladesh. 1st International Conference on Urban and Regional Planning, Bangladesh, 1959: 247–256 (**10 pages**).

Fang, H.; Li, S.; Zhang, Y.; Wei, S.; Wang, Y., (2021). New insights of global vegetation structural properties through an analysis of canopy clumping index, fractional vegetation cover, and leaf area index. Sci. Remote Sens., 4: 10-27 (**18 pages**).

Fashae, O.A.; Adagbasa, E.G.; Olusola, A.O.; Obateru, R.O., (2020). Land use/land cover change and land surface temperature of Ibadan and environs, Nigeria. Environ. Monit. Assess., 192(2): 109 (**18 pages**).

Febrianti, I.; Ridwan, I.; Nurlina, N., (2018). Model SWAT (soil and water assesment tool) untuk analisis erosi dan sedimentasi di catchment area Sungai Besar Kabupaten Banjar. J. Fisika Flux. 15(1): 20-25 (**6 pages**).

Frimawaty, E.; Ilmika, A.; Sakina, N.A; Mustabi. J., (2023). Climate change mitigation and adaptation through livestock waste management. Global J. Environ. Sci. Manage., 9(4): 691-706 **(16 pages).**

García, M.; Moutahir, H.; Casady, G.; Bautista, S.; Rodríguez, F., (2019). Using Hidden Markov Models for land surface phenology: an evaluation across a range of land cover types in Southeast Spain. Remote Sens., 11(5): 507 (**6 pages**).

Gashaw, T.; Bantider, A.; Mahari, A., (2014). Evaluations of land use/land cover changes and land degradation in Dera District, Ethiopia: GIS and remote sensing based analysis. Int. J. Sci. Res. Environ. Sci., 2(6): 199–208 (**10 pages**).

Ghobadi, Y.; Pradhan, B.; Kabiri, K.; Pirasteh, S.; Shafri, H.Z.M.; Sayyad, G.A., (2012). Use of multi-temporal remote sensing data and GIS for wetland change monitoring and degradation. 2012 IEEE Colloquium on Humanities, Science and Engineering . 103–108 (**6 pages**).

Godinho, S.; Gil, A.; Guiomar, N.; Neves, N.; Pinto-Correia, T., (2016). A remote sensing-based approach to estimating montado canopy density using the FCD model: a contribution to identifying HNV farmlands in southern Portugal. Agrofor. Syst., 90(1): 23–34 (**12 pages**).

Guha, S.; Govil, H., (2021). An assessment on the relationship between land surface temperature and normalized difference vegetation index. Environ. Dev. Sustainability. 23(2): 1944–1963 (**20 pages**).

Hu, T.; Liu, J.; Zheng, G.; Zhang, D.; Huang, K., (2020). Evaluation of historical and future wetland degradation using remote sensing imagery and land use modeling. Land Degrad. Dev., 31(1): 65–80 (**16 pages**).

Ibrahim, Y.; Balzter, H.; Kaduk, J.; Tucker, C., (2015). Land degradation assessment using residual trend analysis of GIMMS NDVI3g, soil moisture and rainfall in Sub-Saharan West Africa from 1982 to 2012. Remote Sens., 7(5): 5471–5494 (**24 pages**).

Kadir, S.; Farma, E., (2017). Power recovery support Tabunio watershed based on analysis of erosion based on geographic information system in the province of South Kalimantan. Mediterr. J. Soc. Sci., 8(4–1): 73–81 (**9 pages**).

Kang, H.; Xuxiang, L.; Wang, J.; Zhang, J., (2016). Evaluating ecological vulnerability using the GIS and analytic hierarchy process (AHP) method in Yan'an, China. Pol. J. Environ. Stud., 25(2): 599–605 (**7 pages**).

Karaburun, A., (2010). Estimation of C factor for soil erosion modeling using NDVI in Buyukcekmece watershed. Ozean J. Appl. Sci., 3(1): 77–85 (**9 pages**).

Karydas, C.G.; Panagos, P.; Gitas, I.Z., (2014). A classification of water erosion models according to their geospatial characteristics. Int. J. Digital Earth, 7(3): 229–250 (**22 pages**).

Khawaldah, H.A.; Farhan, I.; Alzboun, N.M., (2020). Simulation and prediction of land use and land cover change using GIS, remote sensing and CA-Markov model. Global J. Environ. Sci. Manage., 6(2): 215–232 (**18 pages**).

Kumsa, A.; Assen, M., (2022). A Comprehensive framework for itu next generation pons. J. Electrical Electron Eng., 1(1): 1–23 (**23 pages**).

Liping, C.; Yujun, S.; Saeed, S., (2018). Monitoring and predicting land use and land cover changes using remote sensing and GIS techniques—A case study of a hilly area, Jiangle, China. PLOS ONE, 13(7): e0200493 (**23 pages**).

Loi, D.T.; Chou, T.-Y.; Fang, Y.-M., (2017). Integration of GIS and remote sensing for evaluating forest canopy density index in Thai Nguyen Province, Vietnam. Int. J. Environ. Sci. Dev., 8(8): 539–542 (**4 pages**).

Loukrakpam, C.; Oinam, B., (2021). Linking the past, present and future scenarios of soil erosion modeling in a river basin. Global J. Environ. Manage, 7(3): 457–472 (**16 pages**).

Ly, K.; Metternicht, G.; Marshall, L., (2019). Transboundary river catchment areas of developing countries: Potential and limitations of watershed models for the simulation of sediment and nutrient loads. A review. J. Hydrol. Reg. Stud., 24100605 (**14 pages**).

Mariye, M.; Mariyo, M.; Changming, Y.; Teffera, Z.L.; Weldegebrial, B., (2022). Effects of land use and land cover change on soil erosion potential in Berhe district: a case study of Legedadi watershed, Ethiopia. Int. J. River Basin Manage., 20(1): 79–91 (**13 pages**).

MohanRajan, S.N.; Loganathan, A., (2021). Modelling spatial drivers for LU/LC change prediction using hybrid machine learning methods in Javadi Hills, Tamil Nadu, India. J. Indian Soc. Remote Sens., 49(4): 913–934 (**22 pages**).

Moonrut, N.; Takrattanasaran, N.; Khamkajorn, T.; Chaikaew, P., (2021). Integrated remote sensing and GIS approaches for land degradation neutrality (LDN) assessment in the agricultural area. IOP Conference Series: Earth Environ. Sci., 626(1): 12-25 (**14 pages**).

Nurlina; Kadir, S.; Kurnain, A.; Ilham, W., (2021). Comparison of maximum likelihood and support vector machine classifiers for land use/land cover mapping using multitemporal imagery 12: 126–139 (1**4 Pages**).

Nurlina; Kadir, S.; Kurnain, A.; Ilham, W.; Ridwan, I., (2022). Analysis of soil erosion and its relationships with land use/cover in Tabunio watershed. IOP Conference Series: Earth Environ. Sci, 976(1): 012027 (**15 pages**).

Nurlina, N.; Kadir, S.; Kurnain, A.; Ilham, W.; Ridwan, I., (2023). Impact of land cover changing on wetland surface temperature based on multitemporal remote sensing data. Pol. J. Environ. Stud., 32(3): 2281–2291 (**11 pages**).

Oguz, H.; Zengin, M., (2011). Analyzing land use/land cover change using remote sensing data and landscape structure metrics: A case study of Erzurum, Turkey. Fresenius Environ. Bull., 20(12): 3258–3269 (**12 pages**).

Peng, W.; Wang, J.; Zhang, J.; Zhang, Y., (2020). Soil moisture estimation in the transition zone from the Chengdu Plain region to the Longmen Mountains by field measurements and LANDSAT 8 OLI/TIRS-derived indices. Arab. J. Geosci., 13(4): 168 (**13 pages**).

Perdana, D.; Renaldi, L.; Alinursafa, I., (2020). Performance analysis of soil moisture monitoring based on internet of things with LoRA communications. J. Southwest Jiaotong Uni., 55(5): 55–64 (**10 pages**).

Pratt, C.R.; Kaly, U.L.; Mitchell, J., (2004). Manual: How to Use the Environmental Vulnerability Index (EVI) (**98 pages**).

Sar, N.; Chatterjee, S.; Das Adhikari, M., (2015). Integrated remote sensing and GIS based spatial modelling through analytical hierarchy process (AHP) for water logging hazard, vulnerability and risk assessment in Keleghai river basin, India. Model. Earth Syst. Environ., 1(4): 31 (**21 pages**).

Shange, P., (2020). Mapping land degradation using remote sensing data and an unsupervised clustering algorithm in the eThekwini Metropolitan Area. University of Kwazulu-Natal, January.

Solangi, Y.A.; Tan, Q.; Mirjat, N.H.; Ali, S., (2019). Evaluating the strategies for sustainable energy planning in Pakistan: An integrated SWOT-AHP and Fuzzy-TOPSIS approach. J. Cleaner Prod., 236117655 (**37 pages**).

Su Mon, M.; Mizoue, N.; Htun, N.Z.; Kajisa, T.; Yoshida, S., (2012). Estimating forest canopy density of tropical mixed deciduous vegetation using Landsat data: a comparison of three classification approaches. Int. J. Remote Sens., 33(4): 1042–1057 (**16 pages**).

Suharyanto, A.; Maulana, A.; Suprayogo, D.; Devia, Y.P.; Kurniawan, S., (2023). Land surface temperature changes caused by land cover/ land use properties and their impact on rainfall characteristics. Global J. Environ., Sci. Manage., 9(3): 353-372 **(20 pages).**

Sun, Y.-L.; Shan, M.; Pei, X.-R.; Zhang, X.-K.; Yang, Y.-L., (2020). Assessment of the impacts of climate change and human activities on vegetation cover change in the Haihe River basin, China. Phys. Chem. Earth., Parts A/B/C, 115102834 **(25 pages).**

Tadese, M.; Kumar, L.; Koech, R.; Kogo, B.K., (2020). Mapping of land-use/land-cover changes and its dynamics in Awash River Basin using remote sensing and GIS. Remote Sens. Appl.: Soc. Environ., 19100352 (**27 pages**).

Tajudin, N.; Ya'acob, N.; Mohd Ali, D.; Adnan, N.A., (2021). Soil moisture index estimation from landsat 8 images for prediction and monitoring landslide occurrences in Ulu Kelang, Selangor, Malaysia. Int. J. Electr. Comput. Eng., 11(3): 2101-2108 (**8 pages**).

Takrina, N.D.; Chuan O.M.; Afifudin, M.I.; Tristan, L.; Arif, I.; Adiwibowo, A ., (2023). Modeling the tropical fish community related to the land uses and environmental determinants. Global J. Environ. Sci. Manage., 9(3): 515-530 **(16 pages).**

Tolche, A.D.; Gurara, M.A.; Pham, Q.B.; Anh, D.T., (2022). Modelling and accessing land degradation vulnerability using remote sensing techniques and the analytical hierarchy process approach. Geocarto Int., 37(24): 7122–7142 (**21 pages**).

Vaishali, G.; Patil, R.R., (2015). Use of remote sensing, GIS and analytical hierarchy process (AHP) in selection of suitable sites for wildlife habitat. Int. J. Curr. Res., 7(3): 14212–14217 (**6 pages**).

van Lynden, G.W.J.; Mantel, S., (2001). The role of GIS and remote sensing in land degradation assessment and conservation mapping: some user experiences and expectations. Int. J. Appl. Earth Obs. Geoinf., 3(1): 61–68 (**8 pages**).

Wang, J.; Ding, J.; Yu, D.; Teng, D.; He, B.; Chen, X.; Ge, X.; Zhang, Z.; Wang, Y.; Yang, X.; Shi, T.; Su, F., (2020). Machine learning-based detection of soil salinity in an arid desert region, Northwest China: A comparison between Landsat-8 OLI and Sentinel-2 MSI. Sci. Total Environ., 707136092 (**11 pages**).

Wiratmoko, B.; Gunawan, T., (2019). Penerapan citra Sentinel 2A dan sistem informasi geografis untuk pemetaan erosi menggunakan pemodelan Musle di DAS Kaligesing, Purworejo. J. Bumi Indonesia (**10 pages**).

Younis, S.M.Z.; Iqbal, J., (2015). Estimation of soil moisture using multispectral and FTIR techniques. Egypt. J. Remote Sens. Space Sci., 18(2): 151–161 (**11 pages**).

Zhu, L.; Ke, Y.; Hong, J.; Zhang, Y.; Pan, Y., (2022). Assessing degradation of lake wetlands in Bashang Plateau, China based on long-term time series Landsat images using wetland degradation index. Ecol. Indic., 139: 108903 (**12 pages**).

AUTHOR (S) BIOSKETCHES

Ridwan, I., Ph.D., Associate Professor, Geophysics, Lambung Mangkurat University, Jl. Ahmad Yani km 36, Banjarbaru, South Kalimantan, Indonesia.
- Email: *ichsanridwan@ulm.ac.id*
- ORCID: 0000-0002-8739-5038
- Web of Science ResearcherID: GNP-8509-2022
- Scopus Author ID: 24077087200
- Homepage: https://physics.ulm.ac.id/profile/19740707-200212-1-003

Kadir, S., Ph.D., Professor, Forest Faculty, Lambung Mangkurat University, Jl. Ahmad Yani km 36, Banjarbaru, South Kalimantan, Indonesia.
- Email: *syarifuddin.kadir@ulm.ac.id*
- ORCID: 0000-0002-1804-0313
- Web of Science ResearcherID:
- Scopus Author ID: 57130338700
- Homepage: https://scholar.google.co.id/citations?user=dPspPHwAAAAJ&hl=en

Nurlina, N., Ph.D., Assistant Professor, Geophysics, Lambung Mangkurat University, Jl. Ahmad Yani km 36, Banjarbaru, South Kalimantan, Indonesia.
- Email: *nurlina_abdullah@ulm.ac.id*
- ORCID: 0000-0002-9563-1555
- Web of Science ResearcherID: AAU-3158-2021
- Scopus Author ID: 57208673588
- Homepage: https://physics.ulm.ac.id/profile/19760414-200312-2-001

HOW TO CITE THIS ARTICLE

Ridwan, I.; Kadir, S.; Nurlina, N., (2024). Wetland degradation monitoring using multi-temporal remote sensing data and watershed land degradation index. Global J. Environ. Sci. Manage., 10(1): 83-96.

DOI: 10.22034/gjesm.2024.01.07

URL: https://www.gjesm.net/article_706487.html